

## Determining Sigma - Lambda mixing

**R. Horsley<sup>\*a</sup>, J. Najjar<sup>b</sup>, Y. Nakamura<sup>c</sup>, H. Perlt<sup>d</sup>, D. Pleiter<sup>eb</sup>, P. E. L. Rakow<sup>f</sup>, G. Schierholz<sup>g</sup>, A. Schiller<sup>d</sup>, H. Stüben<sup>h</sup> and J. M. Zanotti<sup>i</sup>**

<sup>a</sup> School of Physics and Astronomy, University of Edinburgh, Edinburgh EH9 3FD, UK

<sup>b</sup> Institut für Theoretische Physik, Universität Regensburg, 93040 Regensburg, Germany

<sup>c</sup> RIKEN Advanced Institute for Computational Science, Kobe, Hyogo 650-0047, Japan

<sup>d</sup> Institut für Theoretische Physik, Universität Leipzig, 04109 Leipzig, Germany

<sup>e</sup> JSC, Forschungszentrum Jülich, 52425 Jülich, Germany

<sup>f</sup> Theoretical Physics Division, Department of Mathematical Sciences, University of Liverpool, Liverpool L69 3BX, UK

<sup>g</sup> Deutsches Elektronen-Synchrotron DESY, 22603 Hamburg, Germany

<sup>h</sup> Regionales Rechenzentrum, Universität Hamburg, 20146 Hamburg, Germany

<sup>i</sup> CSSM, School of Chemistry and Physics, University of Adelaide, Adelaide SA 5005, Australia

E-mail: rhorsley@ph.ed.ac.uk

### QCDSF-UKQCD Collaborations

SU(2) isospin breaking effects in baryon octet (and decuplet) masses are due to a combination of up and down quark mass differences and electromagnetic effects. These mass differences are small. Between the Sigma and Lambda the mass splitting is much larger, but this is mostly due to their different wavefunctions. However there is now also mixing between these states. We determine the QCD mixing matrix and hence find the mixing angle and mass splitting.

*The 32nd International Symposium on Lattice Field Theory,  
23-28 June, 2014  
Columbia University New York, NY*

---

\*Speaker.

## 1. Introduction

$SU(2)$  isospin breaking effects in hadron octet (and decuplets) are due to a combination of up and down quark mass differences and electromagnetic effects<sup>1</sup>. The baryon octet is shown in the  $I_3$ – $Y$  plane in Fig. 1. On the baryon octet ‘outer’ ring the effects of  $u$ – $d$  mass differences are very

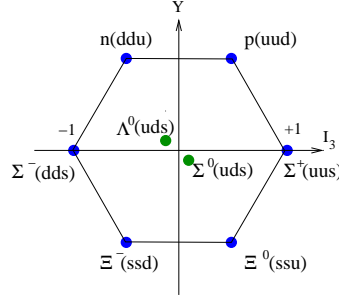


**Figure 1:** The baryon octet in the  $I_3$ – $Y$  plane.

small  $\sim O(\text{few MeV})$ . (The difference in masses between the  $Y = \text{const.}$  particles in this figure.) A compilation of some lattice determinations of these mass splittings is given in the left panel of Fig. 2. However for the Sigma and Lambda baryons, sitting at the centre of the octet, the mass

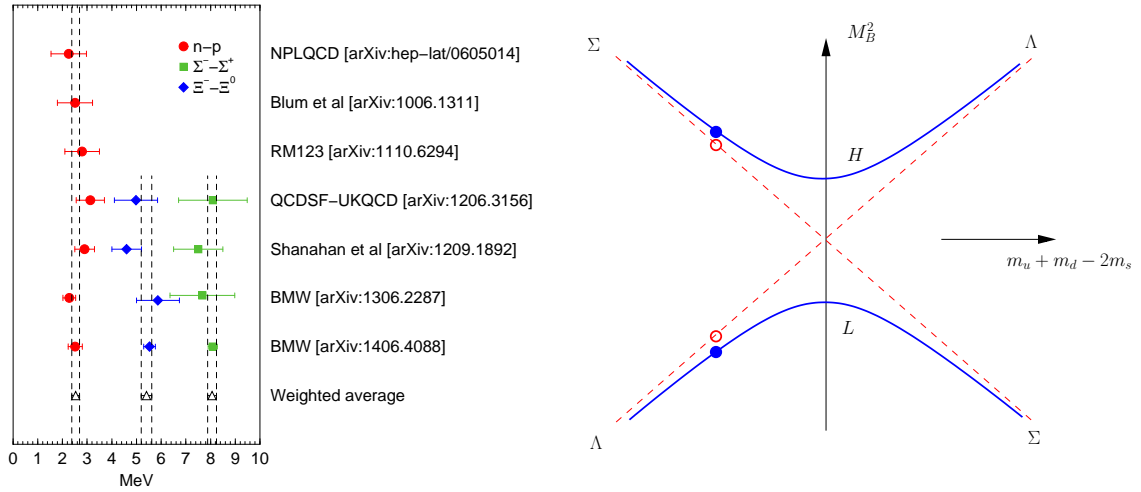


**Figure 2:** Left panel: Lattice determinations for isospin mass breaking due to  $u$ – $d$  quark mass differences for  $n$ – $p$ ,  $\Sigma^-$ – $\Sigma^+$  and  $\Xi^+$ – $\Xi^0$ , together with a weighted average. Right panel: A sketch of the heavy,  $H$ , and light,  $L$ , baryon (masses)<sup>2</sup> against  $m_u + m_d - 2m_s$  for fixed  $m_u - m_d$ . The mass splitting between the Sigma and Lambda masses in the isospin limit ( $m_u = m_d$ ) is given by the difference between the (red) dashed lines; if  $m_u \neq m_d$  then there is an additional mass difference due to mixing, as given by the (blue) lines. The physical point is indicated by the filled (blue) circles.

splitting is much larger,  $(M_{\Sigma^0} - M_{\Lambda^0})^{\text{exp}} = 76.959(23) \text{ MeV}$ . This is mainly due to their different

<sup>1</sup>QED effects will not be considered here.

wavefunctions. However despite the fact that both particles have the same quark content ( $u, d, s$ ) there is also a small additional isospin component due to mixing between these states when the  $u$  and  $d$  quarks have different masses, as depicted in the right panel of Fig. 2. We have the situation of ‘avoided level crossing’. All lines are at constant  $m_u - m_d$ , the (red) dashed lines are for the isospin limit  $m_u = m_d$ , while the (blue) lines are for the case  $m_u - m_d \neq 0$ . The centre point is when all quark masses are the same. We denote the two branches by ‘H’ and ‘L’. The mass splitting between the Sigma and Lambda particles is given by the vertical difference between these points.

In this talk we determine the  $\Sigma$ – $\Lambda$  mixing matrix and hence find the mixing angle and mass splitting. Further details and results are given in [1].

## 2. Method

The strategy we employ here has been described in [2, 3]; we shall extend it here to cover the mixing case. Briefly, in lattice simulations and in particular for the case considered here of three flavours there are many paths for the quark masses to approach the physical point. We have chosen here to extrapolate from a point on the  $SU(3)$  flavour symmetry line (when all the quark masses are equal to  $m_0$  say) to the physical point. As will shortly be seen it is sufficient to consider this for the case of degenerate  $u$  and  $d$  quark masses, i.e.  $m_u = m_d \equiv m_l$  together with the strange quark mass  $m_s$ . Thus we take  $(m_0, m_0) \rightarrow (m_l^*, m_s^*)$ , where a  $*$  denotes the physical point. To define the path the choice here is to keep the singlet quark mass  $\bar{m}$  constant, where  $\bar{m} = m_0 = \frac{1}{3}(2m_l + m_s)$ , along the trajectory. We now develop the  $SU(3)$  flavour symmetry breaking Taylor expansion for hadron masses beginning at the flavour symmetric point in terms of

$$\delta m_q = m_q - \bar{m}. \quad (2.1)$$

The expansion coefficients are functions of  $\bar{m}$  alone and the path is called the ‘unitary line’ as we expand in both sea and valence quarks with the same masses. Thus provided  $\bar{m}$  is kept constant, then the expansion coefficients in the Taylor expansion remain unaltered whether we consider  $2 + 1$  or  $1 + 1 + 1$  flavours, i.e. mass degenerate  $u$  and  $d$  quark masses or not. This opens the possibility of determining quantities that depend on  $1 + 1 + 1$  flavours from just  $2 + 1$  flavour simulations.

Furthermore we can generalise the  $SU(3)$  flavour breaking expansion to the case of partially quenched, PQ, valence quark masses,  $\mu_q$  (with possibly different masses to the sea quark masses  $m_q$ ) without increasing the number of expansion coefficients<sup>2</sup>. Equivalently to eq. (2.1) we set

$$\delta \mu_q = \mu_q - \bar{m}. \quad (2.2)$$

We now define a quark mass matrix  $\mathcal{M}$  and baryon mass matrix  $M(\mathcal{M})$  where

$$\mathcal{M} = \begin{pmatrix} m_u & 0 & 0 \\ 0 & m_d & 0 \\ 0 & 0 & m_s \end{pmatrix}, \quad M^2(\mathcal{M}) = \begin{pmatrix} M_n^2 & 0 & 0 & 0 & 0 & 0 & 0 & 0 \\ 0 & M_p^2 & 0 & 0 & 0 & 0 & 0 & 0 \\ 0 & 0 & M_{\Sigma^-}^2 & 0 & 0 & 0 & 0 & 0 \\ 0 & 0 & 0 & M_{\Sigma\Sigma}^2 & M_{\Sigma\Lambda}^2 & 0 & 0 & 0 \\ 0 & 0 & 0 & M_{\Lambda\Sigma}^2 & M_{\Lambda\Lambda}^2 & 0 & 0 & 0 \\ 0 & 0 & 0 & 0 & 0 & M_{\Sigma^+}^2 & 0 & 0 \\ 0 & 0 & 0 & 0 & 0 & 0 & M_{\Xi^-}^2 & 0 \\ 0 & 0 & 0 & 0 & 0 & 0 & 0 & M_{\Xi^0}^2 \end{pmatrix}, \quad (2.3)$$

<sup>2</sup>The advantage of using PQ valence quarks is that they are computationally cheaper.

and demand<sup>3</sup> that under all  $SU(3)$  transformations

$$\mathcal{M} \rightarrow \mathcal{M}' = U \mathcal{M} U^\dagger \quad \leftrightarrow \quad M^2(\mathcal{M}') = U M^2(\mathcal{M}) U^\dagger. \quad (2.4)$$

Mathematically under these transformations there is no change to the eigenvalues; physically there is also no change, possibly just a relabelling (e.g.  $m_d \leftrightarrow m_s$  is equivalent to relabelling  $M_n \leftrightarrow M_{\Xi^0}, \dots$ ). We write  $M^2 = \sum_{i=1}^{10} K_i(m_q, \mu_q) N_i$ , where the  $N_i$  matrices are classified under  $S_3$  and  $SU(3)$  symmetry and the  $K(m_q, \mu_q)$  are coefficients. The  $S_3$  symmetry group is that of the (equilateral triangle  $C_{3v}$ ) and has 3 irreducible representations: two singlets  $A_1, A_2$  and one doublet  $E$  with elements  $E^\pm$ . The  $N_i$  are mostly diagonal, e.g.  $N_1 = \text{diag}(1, 1, 1, 1, 1, 1, 1, 1)$ , except  $N_5, N_8, N_{10}$ , where the  $\Sigma - \Lambda$   $2 \times 2$  sub-matrices are non-diagonal. Further details of the diagonal matrices are given in [2]; the complete set is described in [1].

This gives for baryons,  $B(aab)$  with valence quarks  $a, b, c$  on the outer ring of the octet

$$M_B^2 = P_{A_1} + P_{E^+}, \quad (2.5)$$

and for the baryons  $B(abc)$  at the centre of the octet (i.e. the  $2 \times 2$  submatrix in  $M^2$  in eq. (2.3))

$$\begin{pmatrix} M_{\Sigma\Sigma}^2 & M_{\Sigma\Lambda}^2 \\ M_{\Lambda\Sigma}^2 & M_{\Lambda\Lambda}^2 \end{pmatrix} = P_{A_1} \begin{pmatrix} 1 & 0 \\ 0 & 1 \end{pmatrix} + P_{E^+} \begin{pmatrix} 1 & 0 \\ 0 & -1 \end{pmatrix} + P_{E^-} \begin{pmatrix} 0 & 1 \\ 1 & 0 \end{pmatrix} + P_{A_2} \begin{pmatrix} 0 & -i \\ i & 0 \end{pmatrix}. \quad (2.6)$$

The  $P_G$  are functions of the quark masses with the symmetry  $G$  under the  $S_3$  permutation group and are given to NLO as

$$\begin{aligned} P_{A_1} &= M_0^2 + 3A_1 \delta\bar{\mu} \\ &\quad + \frac{1}{6}B_0(\delta m_u^2 + \delta m_d^2 + \delta m_s^2) + B_1(\delta\mu_a^2 + \delta\mu_b^2 + \delta\mu_c^2) \\ &\quad + \frac{1}{4}(B_3 + B_4) [(\delta\mu_c - \delta\mu_a)^2 + (\delta\mu_c - \delta\mu_b)^2 + (\delta\mu_a - \delta\mu_b)^2] + O(3) \\ P_{E^+} &= \frac{3}{2}A_2(\delta\mu_c - \delta\bar{\mu}) \\ &\quad + \frac{1}{2}B_2(2\delta\mu_c^2 - \delta\mu_a^2 - \delta\mu_b^2) \\ &\quad + \frac{1}{4}(B_3 - B_4) [(\delta\mu_c - \delta\mu_a)^2 + (\delta\mu_c - \delta\mu_b)^2 - 2(\delta\mu_a - \delta\mu_b)^2] + O(3) \\ P_{E^-} &= \frac{\sqrt{3}}{2}A_2(\delta\mu_b - \delta\mu_a) \\ &\quad + \frac{\sqrt{3}}{2}B_2(\delta\mu_b^2 - \delta\mu_a^2) + \frac{\sqrt{3}}{4}(B_3 - B_4) [(\delta\mu_c - \delta\mu_b)^2 - (\delta\mu_c - \delta\mu_a)^2] + O(3) \\ P_{A_2} &= 0 + O(3), \end{aligned} \quad (2.7)$$

where  $\delta\bar{\mu} = (\delta\mu_a + \delta\mu_b + \delta\mu_c)/3$ . NNLO, i.e.  $O(3)$  terms, have also been determined, [1]. Diagonalisation of eq. (2.6) yields

$$M_H^2 = P_{A_1} + \sqrt{P_{E^+}^2 + P_{E^-}^2 + P_{A_2}^2}, \quad M_L^2 = P_{A_1} - \sqrt{P_{E^+}^2 + P_{E^-}^2 + P_{A_2}^2}. \quad (2.8)$$

Although looking rather complicated, in the isospin limit when there is no mixing, these expansions reduce to those given in [2]. Writing the eigenvectors as  $e_H = (\cos \theta, e^{-i\phi} \sin \theta)$  and  $e_L = (-e^{i\phi} \sin \theta, \cos \theta)$  gives for the mixing angle  $\theta$ , and phase,  $\phi$

$$\tan 2\theta = \frac{\sqrt{P_{E^-}^2 + P_{A_2}^2}}{P_{E^+}}, \quad \tan \phi = \frac{P_{A_2}}{P_{E^-}}, \quad (2.9)$$

<sup>3</sup>The  $SU(3)$  flavour breaking expansion holds for any function of the baryon mass matrix; we have found that using  $M_B^2$  gives slightly better fits than  $M_B$  alone.

and close to the physical point we set  $M_{\Sigma^0} = M_H$ ,  $M_{\Lambda^0} = M_L$  (and  $\theta_{\Sigma^0\Lambda^0} = \theta$ ).

Practically, when analysing the raw lattice results for the baryon masses, it is better to use scale invariant ratios, which helps to make the data smoother. We define the scale implicitly using singlet quantities  $X_S$ ,  $S = \pi, N, \dots$ . For the octet baryons it is convenient to define a ‘centre of mass’ quantity

$$\begin{aligned} X_N^2 &= \frac{1}{6}(M_p^2 + M_n^2 + M_{\Sigma^+}^2 + M_{\Sigma^-}^2 + M_{\Xi^0}^2 + M_{\Xi^-}^2) \\ &= M_0^2 + \frac{1}{6}(B_0 + B_1 + B_3)(\delta m_u^2 + \delta m_d^2 + \delta m_s^2) + O(3). \end{aligned} \quad (2.10)$$

Experimentally  $X_N^{\text{exp}} = 1.160 \text{ GeV}$ . All singlet quantities have no  $O(\delta m_q)$  terms and we have seen [2] that they remain constant down to the physical point, enabling a reliable determination of the scale. It is convenient to form dimensionless ratios within a multiplet

$$\tilde{M}^2 \equiv \frac{M^2}{X_S^2}, \quad S = \pi, N, \dots, \quad \tilde{A}_i \equiv \frac{A_i}{M_0^2}, \quad \tilde{B}_i \equiv \frac{B_i}{M_0^2}, \quad (2.11)$$

and use this in the Taylor expansions.

For example this gives for  $\Sigma - \Lambda$  mixing at LO in the unitary limit, the analytic results

$$\tilde{M}_{\Sigma^0} - \tilde{M}_{\Lambda^0} = \sqrt{\frac{3}{2}} \tilde{A}_2 \sqrt{\delta m_u^2 + \delta m_d^2 + \delta m_s^2}, \quad \tan 2\theta = \frac{(\delta m_d - \delta m_u)}{\sqrt{3} \delta m_s}. \quad (2.12)$$

This shows clearly that any mass difference is dominated by the  $\tilde{A}_2$  coefficient as the  $\tilde{A}_1$  terms have cancelled. This is different to the baryons on the outer ring, which are a mixture of the  $\tilde{A}_1$  and  $\tilde{A}_2$  coefficients (and the numerical values mean that it is actually dominated by the  $\tilde{A}_1$  coefficient). Note also that in the isospin limit where there is no mixing, the mass square root in eq. (2.12) simplifies considerably to give  $\sqrt{6} \delta m_l$ .

### 3. Results

We use here an  $O(a)$  NP improved clover action with tree level Symanzik glue and mildly stout smeared  $2 + 1$  clover fermions, [4], at  $\beta = 5.50$  on  $32^3 \times 64$  and  $48^3 \times 96$  sized lattices. We have found that  $\kappa_0 = 0.12090$  provides a suitable starting point on the  $SU(3)$  symmetric line. The quark mass (whether valence or unitary) is defined as  $\mu_q = (1/\kappa_q - 1/\kappa_{0c})/2$ , where  $\kappa_{0c}$  is the critical  $\kappa_0$  in the chiral limit along the  $SU(3)$  symmetric line. However this does not need to be determined as in  $\delta\mu_q$  it cancels.

The method is first to determine the physical quark masses using the pion octet and equivalent expansions to those described above (and of course only considering pseudoscalar particles on the outer ring), by fitting to unitary and PQ data. This is described in [3] and we also use the results from there. We then for the baryon octet use the unitary and PQ data to determine the  $\tilde{A}$  and  $\tilde{B}$  coefficients. To be sure that the  $SU(3)$  flavour expansion is valid we restrict quark masses to a range here taken to be  $|\delta\mu_a| + |\delta\mu_b| + |\delta\mu_c| \lesssim 0.2$ . This translates to nucleon masses of  $\lesssim 2 \text{ GeV}$ . (In fits it was then found that  $\tilde{B}_3$  was then compatible with zero.) Two simple plots which illustrate the situation are the completely mass degenerate case when  $\Sigma$  and  $\Lambda$  are the same

$$S_{\Sigma\Lambda} \equiv \tilde{M}_{\Sigma}^2(aad'') = 1 + 3\tilde{A}_1 \delta\mu_a + 3\tilde{B}_1 \delta\mu_a^2, \quad (3.1)$$

( $a''$  is a mass degenerate but distinct quark) and the ‘symmetric’ difference case (between  $\Sigma$  and  $\Lambda$ )

$$D_{\Sigma\Lambda}^{\text{sym}} \equiv \frac{\tilde{M}_{\Sigma}^2(aab) - \tilde{M}_{\Lambda}^2(aa'b) - \tilde{M}_{\Sigma}^2(bba) + \tilde{M}_{\Lambda}^2(bb'a)}{4(\delta\mu_b - \delta\mu_a)} = \tilde{A}_2 + \tilde{B}_2(\delta\mu_a + \delta\mu_b), \quad (3.2)$$

as shown in Fig. 3. For  $S_{\Sigma\Lambda}$ , the fit is very good and could be easily extended. As mentioned before

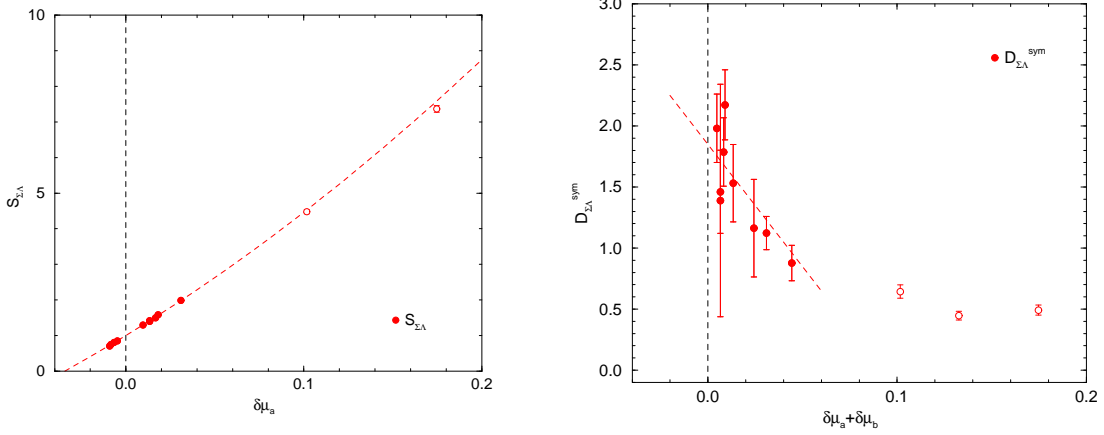


**Figure 3:** Left panel:  $S_{\Sigma\Lambda}$  from eq. (3.1). Right panel:  $D_{\Sigma\Lambda}^{\text{sym}}$  from eq. (3.2). Both are plotted against  $\delta\mu_a + \delta\mu_b$ . Points used in the fit are denoted by filled circles.

$\tilde{A}_1$  is the relevant coefficient for mass splittings on the outer baryon ring. For  $D_{\Sigma\Lambda}^{\text{sym}}$  the symmetric difference is chosen in order to minimise possible effects of terms involving  $\delta\mu_a - \delta\mu_b$ . The plot has a sharp increase as the quark mass is reduced, and presumably a non-polynomial behaviour there. As this is related to the  $\Sigma$ – $\Lambda$  mass splitting, this necessitates a restricted fit region. (It should be noted that the unitary quark masses have  $|\delta m_a| \lesssim 0.01$ .) The reason for this behaviour is due to spin–spin interaction between the quarks. From the Dirac equation we expect the magnetic moment to be  $\propto 1/m_a$ , which might suggest a spin–spin interaction of the form  $\propto 1/(m_a m_b)$ . This has also recently been proposed in [5].

Secondly we show a ‘fan’ plot for the 2 + 1 flavour case:  $\tilde{M}_N^2(aab)$ ,  $\tilde{M}_{\Lambda}^2(aa'b)$ , in Fig. 4. We have  $N(lll'') [= \Lambda_{3l}(ll'l'')]$ ,  $\Sigma(lls)$ ,  $\Xi(ssl)$ ,  $N_s(sss'') [= \Lambda_{3s}(ss's'')]$  and  $\Lambda(ll's)$ ,  $\Lambda_{l2s}(ss'l)$ . ( $N_s(sss'')$  and  $\Lambda_{l2s}(ss'l)$  are fictitious baryons, but provide additional useful data for the fits.) As this is the diagonal case there is no mixing and from eqs. (2.5), (2.8)  $\tilde{M}_N^2 = P_{A_1} + P_{E^+}$ ,  $\tilde{M}_{\Lambda}^2 = P_{A_1} - P_{E^+}$ . We find good agreement with the expected ‘physical’ results.

For baryons on the outer ring of the octet we find that the central values of the mass splittings are in good agreement with previous results, [3] (see also the left panel of Fig. 2), however with an increased error bar. This is the result of the situation depicted in Fig. 3 where previously as shown in the left panel plot, we were able to use a larger fit range. For  $\Sigma^0$  and  $\Lambda^0$  we find

$$M_{\Sigma^0} - M_{\Lambda^0} = 79.44(7.37)(3.37) \text{ MeV}, \quad \tan 2\theta_{\Sigma^0\Lambda^0} = 0.0123(45)(25). \quad (3.3)$$

As anticipated, this gives a very small  $\theta_{\Sigma^0\Lambda^0} \lesssim 1^\circ$ . Taking the difference between the  $M_{\Sigma^0} - M_{\Lambda^0}$  and  $M_{\Sigma}^*(lls) - M_{\Lambda}^*(lls)$  gives the contribution due to isospin breaking of  $\sim 0.01$  MeV.

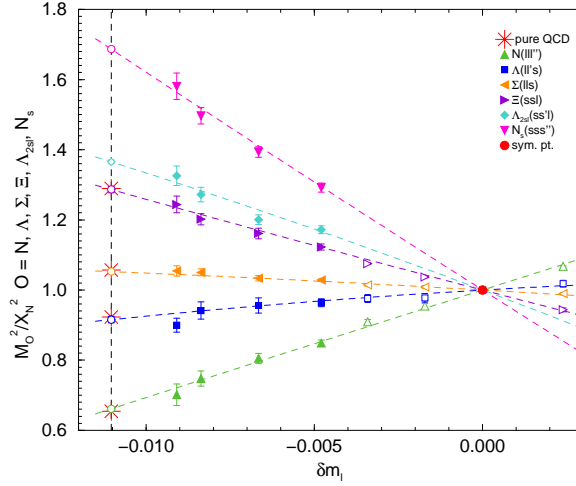


**Figure 4:** The baryon ‘fan’ plot for the ‘N’ and ‘Λ’ type particles  $\tilde{M}_{N_O}^2$  ( $N_O = N, \Sigma, \Xi, N_s$ ) and  $\tilde{M}_{\Lambda_O}^2$  ( $\Lambda_O = N, \Lambda, \Lambda_{I2s}, N_s$ ) versus  $\delta m_l$ . The symbols are all unitary data. (The opaque triangular symbols are from comparison  $24^3 \times 48$  sized lattices and not used in the fits here.) The common symmetric point is the filled circle. The vertical dashed line is the  $N_f = 2 + 1$  pure QCD physical point, with the opaque circles being the numerically determined pure QCD hadron mass ratios for  $2 + 1$  quark flavours. For comparison, the stars represent the average of the  $(\text{mass})^2$  of  $M_N^{*2}(III'') = (M_n^{\text{exp } 2}(ddu) + M_p^{\text{exp } 2}(uud))/2$ ,  $M_\Lambda^{*2}(II's) = M_{\Lambda^0}^{\text{exp } 2}(uds)$ ,  $M_\Sigma^{*2}(II's) = (M_{\Sigma^-}^{\text{exp } 2}(dds) + M_{\Sigma^+}^{\text{exp } 2}(uus))/2$  and  $M_\Xi^{*2}(ssl) = (M_{\Xi^-}^{\text{exp } 2}(ssd) + M_{\Xi^0}^{\text{exp } 2}(ssu))/2$ .

## Acknowledgements

The numerical configuration generation (using the BQCD lattice QCD program) and data analysis (using the Chroma software library) was carried out on the IBM BlueGene/Q using DIRAC 2 resources (EPCC, Edinburgh, UK), the BlueGene/P and Q at NIC (Jülich, Germany), the SGI ICE 8200 and Cray XC30 at HLRN (Berlin–Hannover, Germany) and on the NCI National Facility in Canberra, Australia (supported by the Australian Commonwealth Government). This investigation has been supported partly by the EU grants 227431 (Hadron Physics2) and 283826 (Hadron Physics3). JN was partially supported by EU grant 228398 (HPC-EUROPA2). HP was supported by DFG Grant: SCHI 422/9-1. JMZ was supported by the Australian Research Council grants FT100100005 and DP140103067. We thank all funding agencies.

## References

- [1] R. Horsley *et al.* [QCDSF–UKQCD Collaboration], Phys. Rev. D **91** (2015) 074512, [arXiv:1411.7665[hep-lat]].
- [2] W. Bietenholz *et al.* [QCDSF–UKQCD Collaboration], Phys. Rev. D **84** (2011) 054509, [arXiv:1102.5300[hep-lat]].
- [3] R. Horsley *et al.* [QCDSF–UKQCD Collaboration], Phys. Rev. D **86** (2012) 114511, [arXiv:1206.3156[hep-lat]].
- [4] N. Cundy *et al.* [QCDSF–UKQCD Collaboration], Phys. Rev. D **79** (2009) 094507, [arXiv:0901.3302[hep-lat]].
- [5] Y.-B. Yang *et al.* [ $\chi$ QCD Collaboration], arXiv:1410.3343[hep-lat].